

## **RADIATION OF A DIPOLE LOCATED ON AXIS OF A SEMITRANSSPARENT DISK**

Vadim A. Kaloshin<sup>1</sup>, Kirill K. Klionovski<sup>2</sup>

<sup>1</sup>Kotelnikov Institute of Radioengineering and Electronics of RAS

<sup>2</sup>JSC «Concern «Morinformsystem-Agat»»

The paper is received on May 20, 2014

**Abstract.** Asymptotic formulas for scattering fields of arbitrarily oriented magnetic and electric dipoles located on axis of a semitransparent disk were obtained using the Kirchhoff approximation and the stationary phase method. Expressions for the front-to-back ratio of magnetic and electric dipoles oriented parallel to the disk were obtained. Optimization of the disk's transparency was performed to reduce the back radiation of a magnetic dipole oriented parallel to the disk. Radiation patterns were calculated using the asymptotic formulas and a numerical solution of a singular integral equation.

**Keywords:** semitransparent disk, spherical wave, electric and magnetic dipole, Kirchhoff approximation, stationary phase method.

### **Introduction**

Dipole, monopole and patch antennas are mounted on a perfectly conducting disk to reduce the back lobe [1-22]. Asymptotic formulas for a scattering field of arbitrarily oriented electric and magnetic dipoles located on axis of a perfectly conducting disk were obtained in [22]. A semitransparent disk can be used to decrease the back lobe and the front-to-back ratio in comparison with a perfectly conducting disk of the same radius. Asymptotic expressions for a scattering field of a plane wave by an isotropic resistive semitransparent disk are available in [23]. Scattering of an electric monopole field by an isotropic resistive semitransparent disk was researched numerically in [24]. Scattering of a patch antenna field by a semitransparent disk with anisotropic inductive impedance was considered in [25] using numerical solving of an integral equation. In papers [24, 25] distributions of

transparency were synthesized to decrease the back lobe of the antennas on a semitransparent disk in comparison with the same antenna on a perfectly conducting disk of the same radius.

The first purpose of the present paper is to derive asymptotic expressions for scattering fields of electric and magnetic dipoles located on axis of a semitransparent disk. The second one is to find an optimal transparency of a disk using asymptotic expressions to minimize the back radiation of a magnetic dipole oriented parallel to the disk. The numerical solution of this problem is used to check the accuracy of the asymptotic solutions.

Let us consider a dipole oriented parallel and normally to the disk (Fig. 1). It is enough to determine the field of the arbitrarily oriented dipole. The semitransparent disk is characterized by reflection coefficients  $\eta_\rho^H(\rho)$ ,  $\eta_\phi^H(\rho)$  and transmission coefficients  $\tau_\rho^H(\rho)$ ,  $\tau_\phi^H(\rho)$  for meridional and azimuthal polarization of a magnetic field, respectively. In general case this coefficients depend on radial coordinate  $\rho$  and

the incidence angle  $\theta_{inc}(\rho) = \frac{\pi}{2} + \arctan\left(\frac{h}{\rho}\right)$ . In this paper we assume that

$$|\eta_\phi^H(\rho)|^2 + |\tau_\phi^H(\rho)|^2 \leq 1 \text{ and } |\eta_\rho^H(\rho)|^2 + |\tau_\rho^H(\rho)|^2 \leq 1.$$

In the paper [21] it was shown that the Kirchhoff approximation provides a good agreement with the exact solution for a scattering field of a magnetic current ring mounted on a perfectly conducting disk. Therefore, we use the Kirchhoff approximation to determine the scattering pattern of the dipole located on an axis of a semitransparent disk. The asymptotic expressions for the scattering pattern derived separately near and far from the axis  $Z$ . We use the stationary phase method in a case of stationary point far from end point [26] to evaluate asymptotically the Kirchhoff integral for angles near the axis, and stationary phase method in a case of stationary point near end point [27] for angles far from the axis.

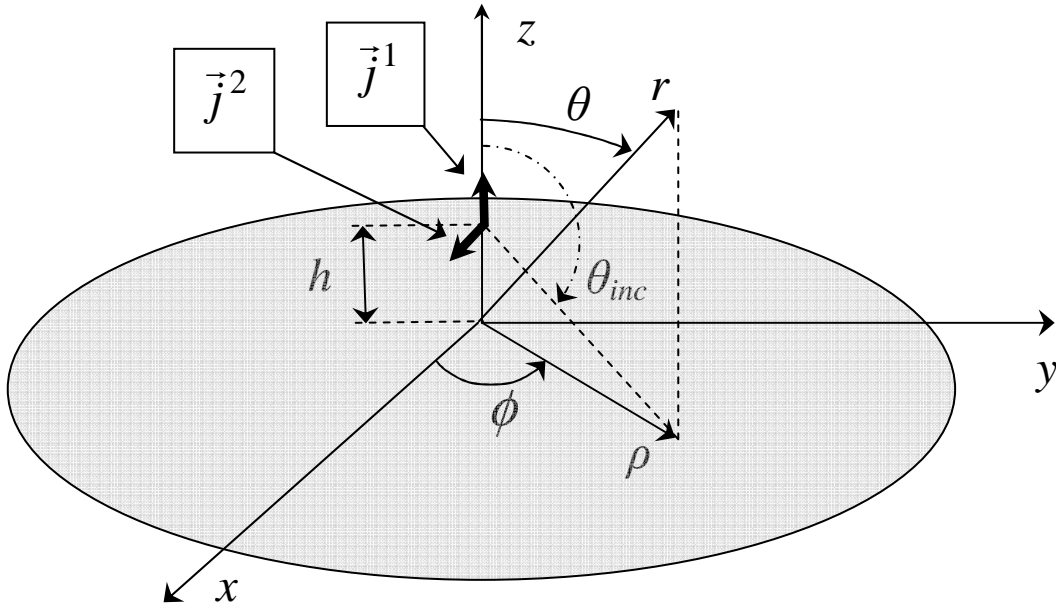


**Fig. 1.** The dipoles on axis of the semitransparent disk

### 1. Fields of the dipoles in free space

Let us consider a perpendicular magnetic dipole

$$\vec{j}_m^1(x, y, z) = m_z \delta(x) \delta(y) \delta(z) \vec{z}_0, \quad (1)$$

and a parallel magnetic dipole

$$\vec{j}_m^2(x, y, z) = m_x \delta(x) \delta(y) \delta(z) \vec{x}_0, \quad (2)$$

where,  $x, y, z$  are Cartesian coordinates;  $\vec{z}_0$  and  $\vec{x}_0$  are the unit vectors in direction of the Z-axis and the X-axis, respectively;  $\delta(x)$  – is the Dirac delta function;  $m_z, m_x$  – are moments of the magnetic dipoles.

Radial  $H_r(r, \theta, \phi)$ , meridional  $H_\theta(r, \theta, \phi)$  and azimuthal  $H_\phi(r, \theta, \phi)$  components of magnetic field of the magnetic dipoles in free space are

$$\begin{aligned} H_r(r, \theta, \phi) &= \frac{m_z}{2\pi W_0} \cos \theta \frac{e^{-ikr}}{r^2} \left( 1 + \frac{1}{ikr} \right), \\ H_\theta(r, \theta, \phi) &= i \frac{m_z k}{4\pi W_0} \sin \theta \frac{e^{-ikr}}{r} \left( 1 + \frac{1}{ikr} - \frac{1}{(kr)^2} \right), \end{aligned} \quad (3)$$

$$H_\phi(r, \theta, \phi) = 0,$$

in a case of the perpendicular magnetic dipole, and

$$\begin{aligned}
 H_r(r, \theta, \phi) &= \frac{m_x}{2\pi W_0} \sin \theta \cos \phi \frac{e^{-ikr}}{r^2} \left( 1 + \frac{1}{ikr} \right), \\
 H_\theta(r, \theta, \phi) &= -i \frac{m_x k}{4\pi W_0} \cos \theta \cos \phi \frac{e^{-ikr}}{r} \left( 1 + \frac{1}{ikr} - \frac{1}{(kr)^2} \right), \\
 H_\phi(r, \theta, \phi) &= i \frac{m_x k}{4\pi W_0} \sin \phi \frac{e^{-ikr}}{r} \left( 1 + \frac{1}{ikr} - \frac{1}{(kr)^2} \right),
 \end{aligned} \tag{4}$$

in a case of the parallel magnetic dipole. Here,  $r, \theta, \phi$  are spherical coordinates;  $i = \sqrt{-1}$ ;  $k = 2\pi/\lambda$ ;  $\lambda$  is wavelength;  $W_0 = 120\pi$ .

Let us consider a perpendicular electric dipole

$$\vec{j}_e^1(x, y, z) = p_z \delta(x) \delta(y) \delta(z) \vec{z}_0, \tag{5}$$

and a parallel electric dipole

$$\vec{j}_e^2(x, y, z) = p_x \delta(x) \delta(y) \delta(z) \vec{x}_0. \tag{6}$$

Here,  $p_z, p_x$  – are moments of the electric dipoles. Components of the magnetic field of the perpendicular and parallel electric dipole in free space are respectively

$$\begin{aligned}
 H_r(r, \theta, \phi) &= 0, \\
 H_\theta(r, \theta, \phi) &= 0, \\
 H_\phi(r, \theta, \phi) &= i \frac{p_z k}{4\pi} \sin \theta \frac{e^{-ikr}}{r} \left( 1 + \frac{1}{ikr} \right),
 \end{aligned} \tag{7}$$

and

$$\begin{aligned}
 H_r(r, \theta, \phi) &= 0, \\
 H_\theta(r, \theta, \phi) &= -i \frac{p_x k}{4\pi} \sin \phi \frac{e^{-ikr}}{r} \left( 1 + \frac{1}{ikr} \right), \\
 H_\phi(r, \theta, \phi) &= -i \frac{p_x k}{4\pi} \cos \theta \cos \phi \frac{e^{-ikr}}{r} \left( 1 + \frac{1}{ikr} \right).
 \end{aligned} \tag{8}$$

## 2. Scattering field in the Kirchhoff approximation

Let us define the asymptotic expressions for azimuthal  $H_\phi^\Sigma(r, \theta, \phi)$  and meridional  $H_\theta^\Sigma(r, \theta, \phi)$  components of field in far zone of the electric and magnetic

dipoles. The dipoles locate on the axis of the disk of radius  $R$  on distance  $h$  above the disk (Fig. 1). These expressions in the Kirchhoff approximation are

$$H_{\phi}^{\Sigma}(r, \theta, \phi) = H_{\phi}(r, \theta, \phi)e^{ikh\cos\theta} + \int_{\rho=0}^R j_{\rho}^e(\rho, \phi)H_{\phi}^{\rho}(r, \theta, \rho)d\rho +$$

$$+ \int_{\rho=0}^R j_{\phi}^e\left(\rho, \phi - \xi\frac{\pi}{2}\right)H_{\phi}^{\phi}(r, \theta, \rho)d\rho, \quad (9)$$

$$H_{\theta}^{\Sigma}(r, \theta, \phi) = H_{\theta}(r, \theta, \phi)e^{ikh\cos\theta} + \int_{\rho=0}^R j_{\rho}^e\left(\rho, \phi + \xi\frac{\pi}{2}\right)H_{\theta}^{\rho}(r, \theta, \rho)d\rho +$$

$$+ \int_{\rho=0}^R j_{\phi}^e(\rho, \phi)H_{\theta}^{\phi}(r, \theta, \rho)d\rho, \quad (10)$$

In (9), (10) the variable  $\xi = -1$  for the perpendicular magnetic dipole or the parallel electric dipole. The variable  $\xi = 1$  for the parallel magnetic dipole or the perpendicular electric dipole. Radial  $j_{\rho}^e(\rho, \phi)$  and azimuthal  $j_{\phi}^e(\rho, \phi)$  components of an electric current of semitransparent disk are determined using a boundary condition  $\vec{j}^e = [\vec{z}_0, 2\vec{H}]$ :

$$j_{\rho}^e(\rho, \phi) = -2\eta_{\phi}^H(\rho)H_{\phi}\left(\sqrt{\rho^2 + h^2}, \frac{\pi}{2} + \theta^s(\rho), \phi\right),$$

$$j_{\phi}^e(\rho, \phi) = 2\eta_{\rho}^H(\rho)\left[H_r\left(\sqrt{\rho^2 + h^2}, \frac{\pi}{2} + \theta^s(\rho), \phi\right)\cos(\theta^s(\rho)) -$$

$$- H_{\theta}\left(\sqrt{\rho^2 + h^2}, \frac{\pi}{2} + \theta^s(\rho), \phi\right)\sin(\theta^s(\rho))\right], \quad (11)$$

$$\theta^s(\rho) = \arctan\left(\frac{h}{\rho}\right).$$

The radial  $H_r(r, \theta, \phi)$ , meridional  $H_{\theta}(r, \theta, \phi)$  and azimuthal  $H_{\phi}(r, \theta, \phi)$  component in (9)-(11) corresponds to the radial, meridional and azimuthal component in (3), (4), (7) or (8) of analyzed dipole  $\vec{j}_m^1$ ,  $\vec{j}_m^2$ ,  $\vec{j}_e^1$  or  $\vec{j}_e^2$ , respectively. Components of field in far zone of rings of radial and azimuthal electric currents of radius  $\rho$  are

$$\begin{aligned}
 H_{\theta}^{\rho}(r, \theta, \rho) &= \xi n i^n \frac{k\rho}{4} [J_{n-1}(k\rho \sin \theta) + J_{n+1}(k\rho \sin \theta)] \frac{e^{-ikr}}{r}, \\
 H_{\phi}^{\rho}(r, \theta, \rho) &= -i^n \frac{k\rho}{4} \cos \theta [J_{n-1}(k\rho \sin \theta) - J_{n+1}(k\rho \sin \theta)] \frac{e^{-ikr}}{r}, \\
 H_{\theta}^{\phi}(r, \theta, \rho) &= i^n \frac{k\rho}{4} [J_{n-1}(k\rho \sin \theta) - J_{n+1}(k\rho \sin \theta)] \frac{e^{-ikr}}{r}, \\
 H_{\phi}^{\phi}(r, \theta, \rho) &= -\xi n i^n \frac{k\rho}{4} \cos \theta [J_{n-1}(k\rho \sin \theta) + J_{n+1}(k\rho \sin \theta)] \frac{e^{-ikr}}{r}.
 \end{aligned} \tag{12}$$

Here  $J_m(u)$  is the Bessel function of order  $m$ ,  $n=0$  for the perpendicular magnetic and electric dipoles, and  $n=1$  for the parallel magnetic and electric dipoles.

### 3. The asymptotic expressions of field near the axis

We assume that reflection and transmission coefficients are slowly varying functions. We use the stationary phase method [26] in a case of stationary point far from the end point to evaluate asymptotically the integrals (9), (10) near the axis. In this case the contribution of stationary point and the end point calculate apart. The asymptotic expressions of field near the axis are

$$H_{\phi}^{\Sigma}(r, \theta, \phi) = \begin{cases} H_{\phi}(r, \theta, \phi) [e^{ikh \cos \theta} + \xi \eta_{\phi}^H (h \tan \theta) e^{-ikh \cos \theta}] - H_{\phi}^S(r, \theta, \phi), & 0 \leq \theta \leq \frac{\pi}{2}, \\ H_{\phi}(r, \theta, \phi) \tau_{\phi}^H (h \tan(\pi - \theta)) e^{ikh \cos \theta} - H_{\phi}^S(r, \theta, \phi), & \frac{\pi}{2} < \theta \leq \pi \end{cases}, \tag{13}$$

for the azimuthal component of field, and

$$H_{\theta}^{\Sigma}(r, \theta, \phi) = \begin{cases} H_{\theta}(r, \theta, \phi) [e^{ikh \cos \theta} + \xi \eta_{\rho}^H (h \tan \theta) e^{-ikh \cos \theta}] - H_{\theta}^S(r, \theta, \phi), & 0 \leq \theta \leq \frac{\pi}{2}, \\ H_{\theta}(r, \theta, \phi) \tau_{\rho}^H (h \tan(\pi - \theta)) e^{ikh \cos \theta} - H_{\theta}^S(r, \theta, \phi), & \frac{\pi}{2} < \theta \leq \pi \end{cases}, \tag{14}$$

for the meridional component of field. The azimuthal  $H_{\phi}(r, \theta, \phi)$  and meridional  $H_{\theta}(r, \theta, \phi)$  component in (13), (14) corresponds to the azimuthal and meridional component in (3), (4), (7) or (8) of analyzed dipole  $\vec{j}_m^1$ ,  $\vec{j}_m^2$ ,  $\vec{j}_e^1$  or  $\vec{j}_e^2$ , respectively.

Scattering fields in far zone for the angles near the axis in the Kirchhoff approximation are

$$H_{\phi}^S(r, \theta, \phi) = \frac{j_{\rho}^e(R, \phi)H_{\phi}^{\rho}(r, \theta, R) + j_{\phi}^e\left(R, \phi - \xi \frac{\pi}{2}\right)H_{\phi}^{\phi}(r, \theta, R)}{ik \cos(\theta^s(R))},$$

$$H_{\theta}^S(r, \theta, \phi) = \frac{j_{\rho}^e\left(R, \phi + \xi \frac{\pi}{2}\right)H_{\theta}^{\rho}(r, \theta, R) + j_{\phi}^e(R, \phi)H_{\theta}^{\phi}(r, \theta, R)}{ik \cos(\theta^s(R))}.$$
(15)

Let us define the front-to-back ratio  $K_{FB} = \left| \frac{H_{\phi}^{\Sigma}(r \rightarrow \infty, \theta = 0, \phi)}{H_{\phi}^{\Sigma}(r \rightarrow \infty, \theta = \pi, \phi)} \right|$  for parallel

electric and magnetic dipoles in the Kirchhoff approximation using the asymptotic expression (13) near the Z-axis:

$$K_{FB}^m = \left| \frac{e^{ikh} + \eta_{\phi}^H(0)e^{-ikh} - H_{\phi_{-m}}^S}{\tau_{\phi}^H(0)e^{-ikh} + H_{\phi_{-m}}^S} \right|,$$

$$H_{\phi_{-m}}^S = \frac{e^{-ik\sqrt{R^2+h^2}} R}{2 \cos(\theta^s(R))\sqrt{R^2+h^2}} \left( \frac{2i\eta_{\rho}^H(R)(\cos(\theta^s(R)))^2}{k\sqrt{R^2+h^2}} \left( 1 + \frac{1}{ik\sqrt{R^2+h^2}} \right) + \right.$$

$$\left. + \left[ \eta_{\phi}^H(R) + \eta_{\rho}^H(R)(\sin(\theta^s(R)))^2 \right] \left( 1 + \frac{1}{ik\sqrt{R^2+h^2}} - \frac{1}{k^2(R^2+h^2)} \right) \right),$$
(16)

for the parallel magnetic dipole, and

$$K_{FB}^e = \left| \frac{-e^{ikh} + \eta_{\phi}^H(0)e^{-ikh} - H_{\phi_{-e}}^S}{\tau_{\phi}^H(0)e^{-ikh} + H_{\phi_{-e}}^S} \right|,$$

$$H_{\phi_{-e}}^S = \frac{e^{-ik\sqrt{R^2+h^2}} h}{2\sqrt{R^2+h^2}} \left( 1 + \frac{1}{ik\sqrt{R^2+h^2}} \right) \left( \eta_{\phi}^H(R) + \eta_{\rho}^H(R) \right),$$
(17)

for the parallel electric dipole.

#### 4. The asymptotic expressions of field far from the axis

We use the asymptotic representation of the Bessel function in (12) when the argument is large and the stationary phase method [27] in a case of a stationary point

near the end point to evaluate asymptotically the integrals (9), (10) far from the axis.

The asymptotic expressions of field far from the axis are

$$\begin{aligned}
 H_{\phi}^{\Sigma}(r, \theta, \phi) = & H_{\phi}(r, \theta, \phi) \left[ e^{ikh \cos \theta} \chi \left( \frac{\pi}{2} + \theta^s(R) - \theta \right) + \right. \\
 & + \xi \eta_{\phi}^H (h \tan \theta) e^{-ikh \cos \theta} \chi \left( \frac{\pi}{2} - \theta^s(R) - \theta \right) + \\
 & \left. + \tau_{\phi}^H (h \tan(\pi - \theta)) e^{ikh \cos \theta} \chi \left( \theta - \frac{\pi}{2} - \theta^s(R) \right) \right] + \sqrt{\frac{\cos(\theta^s(R))}{\sin \theta}} \eta_{\phi}^H(R) H_{\phi}(r, \theta, \phi) \times \\
 & \times \left( e^{ikh \cos \theta} \left[ F(s_Q^r(\theta)) - \tilde{F}(s_Q^r(\theta)) - (-1)^n i \left( F(s_P^r(\theta)) - \tilde{F}(s_P^r(\theta)) \right) \right] + \right. \\
 & + \xi e^{-ikh \cos \theta} \left[ F(s_Q^m(\theta)) - \tilde{F}(s_Q^m(\theta)) - (-1)^n i \left( F(s_P^m(\theta)) - \tilde{F}(s_P^m(\theta)) \right) \right] \Big) - \\
 & - i^n \frac{\cos \theta}{\sqrt{2\pi k \sin \theta}} \frac{\sqrt{R} \eta_{\phi}^H(R)}{\sqrt{R^2 + h^2}} H_{\phi} \left( r, \frac{\pi}{2} + \theta^s(R), \phi \right) \times \\
 & \times \left[ \frac{e^{ik(R \sin \theta - \sqrt{R^2 + h^2})} e^{-i\left(\frac{\pi}{4} + \frac{n\pi}{2}\right)}}{\cos(\Theta_1(\theta)) + \cos(\theta^s(R))} - \frac{e^{-ik(R \sin \theta + \sqrt{R^2 + h^2})} e^{i\left(\frac{\pi}{4} + \frac{n\pi}{2}\right)}}{\cos(\Theta_2(\theta)) + \cos(\theta^s(R))} \right], \tag{18}
 \end{aligned}$$

for the azimuthal component of field, and

$$\begin{aligned}
 H_{\theta}^{\Sigma}(r, \theta, \phi) = & H_{\theta}(r, \theta, \phi) \left[ e^{ikh \cos \theta} \chi \left( \frac{\pi}{2} + \theta^s(R) - \theta \right) + \right. \\
 & + \xi \eta_{\rho}^H (h \tan \theta) e^{-ikh \cos \theta} \chi \left( \frac{\pi}{2} - \theta^s(R) - \theta \right) + \\
 & \left. + \tau_{\rho}^H (h \tan(\pi - \theta)) e^{ikh \cos \theta} \chi \left( \theta - \frac{\pi}{2} - \theta^s(R) \right) \right] + \sqrt{\frac{\cos(\theta^s(R))}{\sin \theta}} \eta_{\rho}^H(R) H_{\theta}(r, \theta, \phi) \times \\
 & \times \left( e^{ikh \cos \theta} \left[ F(s_Q^r(\theta)) - \tilde{F}(s_Q^r(\theta)) - (-1)^n i \left( F(s_P^r(\theta)) - \tilde{F}(s_P^r(\theta)) \right) \right] + \right. \\
 & + \xi e^{-ikh \cos \theta} \left[ F(s_Q^m(\theta)) - \tilde{F}(s_Q^m(\theta)) - (-1)^n i \left( F(s_P^m(\theta)) - \tilde{F}(s_P^m(\theta)) \right) \right] \Big) + \\
 & + i^n \frac{\sin(\theta^s(R))}{\sqrt{2\pi k \sin \theta}} \frac{\sqrt{R} \eta_{\rho}^H(R)}{\sqrt{R^2 + h^2}} H_{\theta} \left( r, \frac{\pi}{2} + \theta^s(R), \phi \right) \times \\
 & \times \left[ \frac{e^{ik(R \sin \theta - \sqrt{R^2 + h^2})} e^{-i\left(\frac{\pi}{4} + \frac{n\pi}{2}\right)}}{\cos(\Theta_1(\theta)) + \cos(\theta^s(R))} - \frac{e^{-ik(R \sin \theta + \sqrt{R^2 + h^2})} e^{i\left(\frac{\pi}{4} + \frac{n\pi}{2}\right)}}{\cos(\Theta_2(\theta)) + \cos(\theta^s(R))} \right], \tag{19}
 \end{aligned}$$

for the meridional component of field. The azimuthal  $H_\phi(r, \theta, \phi)$  and meridional  $H_\theta(r, \theta, \phi)$  component in (18), (19) corresponds to the azimuthal and meridional component in (3), (4), (7) or (8) of analyzed dipole  $\vec{J}_m^1, \vec{J}_m^2, \vec{J}_e^1$  or  $\vec{J}_e^2$ , respectively.

In (18), (19)  $\chi(z) = \begin{cases} 1, & z \geq 0 \\ 0, & z < 0 \end{cases}$  is the Heaviside function. Function  $\tilde{F}(x) = -\frac{e^{-ix^2}}{2\sqrt{i\pi x}}$  is

the first term of the asymptotic expansion of the Fresnel integral

$$F(x) = -\text{sign}(x) \sqrt{\frac{i}{\pi}} \int_{-\infty}^{-\text{sign}(x)x} e^{-it^2} dt. \text{ The arguments of the functions } F(x) \text{ and } \tilde{F}(x)$$

in (18), (19) are

$$\begin{aligned} s_Q^r(\theta) &= \sqrt{2k\sqrt{R^2 + h^2}} \cos\left(\frac{\Theta_1(\theta) - \theta^s(R)}{2}\right), \\ s_P^r(\theta) &= \sqrt{2k\sqrt{R^2 + h^2}} \cos\left(\frac{\Theta_2(\theta) - \theta^s(R)}{2}\right), \\ s_Q^m(\theta) &= \sqrt{2k\sqrt{R^2 + h^2}} \cos\left(\frac{\Theta_1(\theta) + \theta^s(R)}{2}\right), \\ s_P^m(\theta) &= \sqrt{2k\sqrt{R^2 + h^2}} \cos\left(\frac{\Theta_2(\theta) + \theta^s(R)}{2}\right), \\ \Theta_1(\theta) &= \theta + \frac{\pi}{2}, \quad \Theta_2(\theta) = \begin{cases} \frac{\pi}{2} - \theta, & 0 \leq \theta < \frac{\pi}{2} \\ 2\pi + \frac{\pi}{2} - \theta, & \frac{\pi}{2} \leq \theta \leq \pi \end{cases}. \end{aligned} \quad (20)$$

### 5. The numerical solution of an integral equation

The scattering of a dipole field by the semitransparent disk can be investigated by solving a singular integral equation of the second kind numerically. Consider boundary conditions on the surface of semitransparent disk:

$$\vec{E}_\tau^+ = \vec{E}_\tau^-, \quad [\vec{z}_0 \times (\vec{H}_\tau^+ - \vec{H}_\tau^-)] = \vec{J}_{num}^e, \quad \vec{E}_\tau^+ = \vec{J}_{num}^e \hat{Z}. \quad (21)$$

Here,  $\vec{E}_\tau^+, \vec{H}_\tau^+$  are tangential components of the electric and magnetic fields on the illuminated side of the semitransparent disk;  $\vec{E}_\tau^-, \vec{H}_\tau^-$  are tangential components of

the electric and magnetic fields on the dark side of the semitransparent disk;  $\vec{j}_{num}^e$  is the unknown electric current on the disk; and  $\hat{Z}$  is the impedance tensor with complex components. In the polar coordinates (Fig. 1) the boundary conditions (21) take the form

$$E_{\rho}^+ = E_{\rho}^-, \quad E_{\phi}^+ = E_{\phi}^-, \quad H_{\rho}^+ - H_{\rho}^- = j_{\phi\_num}^e, \quad H_{\phi}^+ - H_{\phi}^- = -j_{\rho\_num}^e. \quad (22)$$

The electric current on the disk is associated with the tangential component of the electric field on the disk's surface through the impedance tensor  $\hat{Z}$  :

$$\begin{pmatrix} E_{\rho}^+ \\ E_{\phi}^+ \end{pmatrix} = \begin{pmatrix} Z_{rr} & 0 \\ 0 & Z_{\phi\phi} \end{pmatrix} \begin{pmatrix} j_{\rho\_num}^e \\ j_{\phi\_num}^e \end{pmatrix}, \quad (23)$$

where  $Z_{rr}(r) = \frac{W_0 \tau_{\phi}^H(r)}{2\eta_{\phi}^H(r)}$ ,  $Z_{\phi\phi}(r) = \frac{W_0 \tau_{\rho}^H(r)}{2\eta_{\rho}^H(r)}$ . Consider the boundary condition

$\vec{E}_{\tau}^+ = \vec{j}_{num}^e \hat{Z}$ . The tangential component of the electric field consist of an electric field of a dipole in free space  $\vec{E}_{\tau}$  and an electric field of the unknown electric current which expresses in terms of a Green's tensor . Thus, we obtain an integral equation of the second kind relative to the unknown electric current of the disk:

$$\int_{S'} \hat{G}(r, \phi, r', \phi') \vec{j}_{num}^e(r', \phi') dS' + \vec{E}_{\tau}(r, \phi) = \hat{Z}(r) \vec{j}_{num}^e(r, \phi). \quad (24)$$

Here,  $\hat{G}$  is the Green's tensor;  $S'$  is the surface of the disk. We use the method of moments and the algorithm described in [21, 22, 25] to solve the integral equation (24). The unknown electric current  $\vec{j}_{num}^e$  shall be decomposed over basis of triangular elements:

$$\vec{j}_{num}^e(r, \phi) = \vec{r}_0 \sum_{n=0}^{N_r} I_n^r \Delta_r(r - r_n, \phi) + \vec{\phi}_0 \sum_{n=0}^{N_{\phi}} I_n^{\phi} \Delta_{\phi}(r - r_n, \phi). \quad (25)$$

Here,  $I_n^r, I_n^{\phi}$  are unknown current amplitudes;  $\vec{r}_0$  is the radial unit vector;  $\vec{\phi}_0$  is the azimuthal unit vector. Basic functions with bases  $2T_r$  and  $2T_{\phi}$  have the form

$$\Delta_r(r - r_n, \phi) = 0,$$

$$\Delta_\phi(r - r_n, \phi) = \left[ 1 - \frac{|r - nT_\phi|}{T_\phi} \right]; \quad (n-1)T_\phi \leq r \leq (n+1)T_\phi, \quad (26)$$

for the perpendicular magnetic dipole, and

$$\Delta_r(r - r_n, \phi) = \left[ 1 - \frac{|r - nT_r|}{T_r} \right] \sin \phi; \quad (n-1)T_r \leq r \leq (n+1)T_r,$$

$$\Delta_\phi(r - r_n, \phi) = \left[ 1 - \frac{|r - nT_\phi|}{T_\phi} \right] \cos \phi; \quad (n-1)T_\phi \leq r \leq (n+1)T_\phi, \quad (27)$$

for the parallel electric and magnetic dipoles. The method of moments reduces the problem of scattering to a system of linear algebraic equations. A matrix of the unknown current's amplitudes can be determined solving this system:

$$\hat{I} = (\hat{W} - \hat{A})^{-1} \hat{U}. \quad (28)$$

Elements of matrix of own and mutual impedances  $\hat{A}$  are calculated by numerical integration of the Green's tensor components  $\hat{G}^{r(\phi), r(\phi)}$  and the basic functions:

$$A_{m,n}^{r(\phi), r(\phi)} = \int_S \Delta_{r(\phi)}(r - r_m, \phi) \int_{S'} \hat{G}^{r(\phi), r(\phi)}(r, \phi, r', \phi') \Delta_{r(\phi)}(r' - r_n, \phi') dS' dS. \quad (29)$$

A representation of components  $\hat{G}^{r(\phi), r(\phi)}$  in spectral form was used during calculations of the own and "nearest" mutual impedances in the matrix  $\hat{A}$ . The basic function was decomposed into a two-dimensional Fourier integral over flat sheets of electric current. Integral over the surface  $S'$  in (29) was determined by integrating fields of the flat sheets with components  $\hat{G}^{r(\phi), r(\phi)}$ . A representation  $\hat{G}^{r(\phi), r(\phi)}$  in source-wise form for a ring of radial and azimuthal current in the spherical coordinates was used for purpose of reducing computation time in calculating the "distant" mutual impedances in the matrix  $\hat{A}$ . Elements of a matrix  $\hat{U}$  which describes an interaction of field of a dipole and the current of the disk have the following form:

$$U_m^{r(\phi)} = \int_S \Delta_{r(\phi)}(r - r_m, \phi) E_\tau(r, \phi) dS. \quad (30)$$

Elements of matrix  $\hat{W}$  are defined as

$$W_{m,n}^{r(\phi),r(\phi)} = \int_S Z_{r(\phi),r(\phi)}(r) \Delta_{r(\phi)}(r-r_m, \phi) \Delta_{r(\phi)}(r-r_n, \phi) dS. \quad (31)$$

The scattering field is determined by summing the field of a dipole (3), (4), (7) or (8), and the field of the electric current of the disk. The field of the disk's electrical current is determined by numerical integration of fields of radial and azimuthal electrical current's rings. The integration was performed over radius of the rings with amplitude distribution (25).

### 6. The numerical and asymptotic research of scattering by the disk

Let us consider a semitransparent disk of radius  $R=2\lambda$  with magnitudes and arguments of the reflection and transmission coefficients  $\eta_\rho^H(\rho) = \eta_\phi^H(\rho)$  and  $\tau_\rho^H(\rho) = \tau_\phi^H(\rho) = 1 - \eta_\rho^H(\rho)$  which are shown in fig. 2. The components  $Z_{rr}(r) = Z_{\phi\phi}(r)$  of impedance tensor (23) are shown in fig. 3. These components are normalized to  $W_0$ .

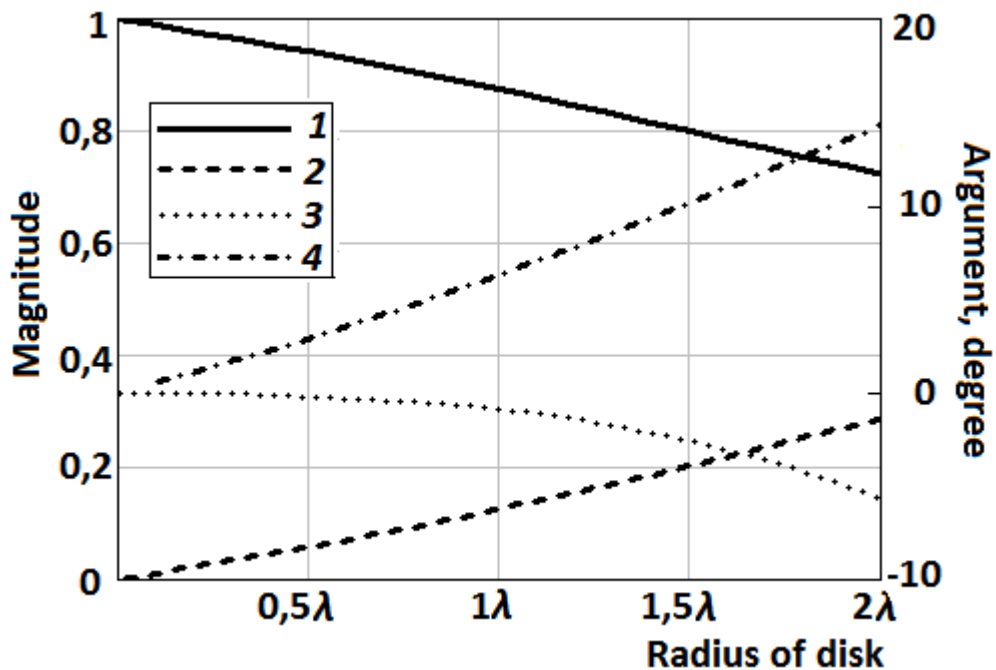


**Fig. 2.** The distribution of magnitudes and arguments of the reflection and transmission coefficients: 1 – magnitude of the reflection coefficient; 2 – magnitude

of the transmission coefficient; 3 – argument of the reflection coefficient; 4 – argument of the transmission coefficient

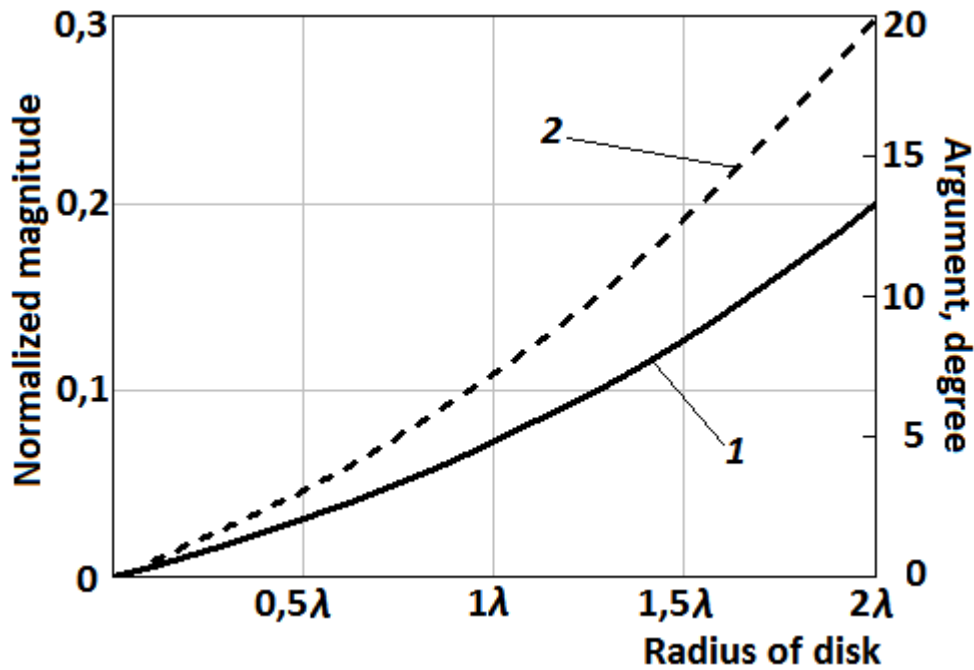


**Fig. 3.** The distribution of components of the impedance tensor (23) on the disk's surface: 1 – normalized magnitude of the impedance; 2 – argument of the impedance

Numerical results obtained using the numerical solution of the integral equation, the numerical integration of the Kirchhoff integral (formulas (9) and (10)) and the asymptotic formulas (13), (14), (18), (19) are shown in fig. 4 – 9. Figures 4 and 5 show patterns of the parallel magnetic dipole mounted on the disk in  $E$ -plane  $H_{\phi}^{\Sigma}\left(r, \theta, \phi = \frac{\pi}{2}\right)$  and  $H$ -plane  $H_{\theta}^{\Sigma}(r, \theta, \phi = 0)$ , respectively. Figures 6 and 7 show patterns of the parallel electric dipole located on distance  $h=2\lambda$  above the disk in  $E$ -plane  $H_{\phi}^{\Sigma}(r, \theta, \phi = 0)$  and  $H$ -plane  $H_{\theta}^{\Sigma}\left(r, \theta, \phi = \frac{\pi}{2}\right)$ , respectively. Figure 8 shows patterns  $H_{\theta}^{\Sigma}(r, \theta, \phi)$  of the perpendicular magnetic dipole located on distance  $h=1.5\lambda$  above the disk. Figure 9 shows patterns  $H_{\phi}^{\Sigma}(r, \theta, \phi)$  of the perpendicular electric dipole mounted on the disk.

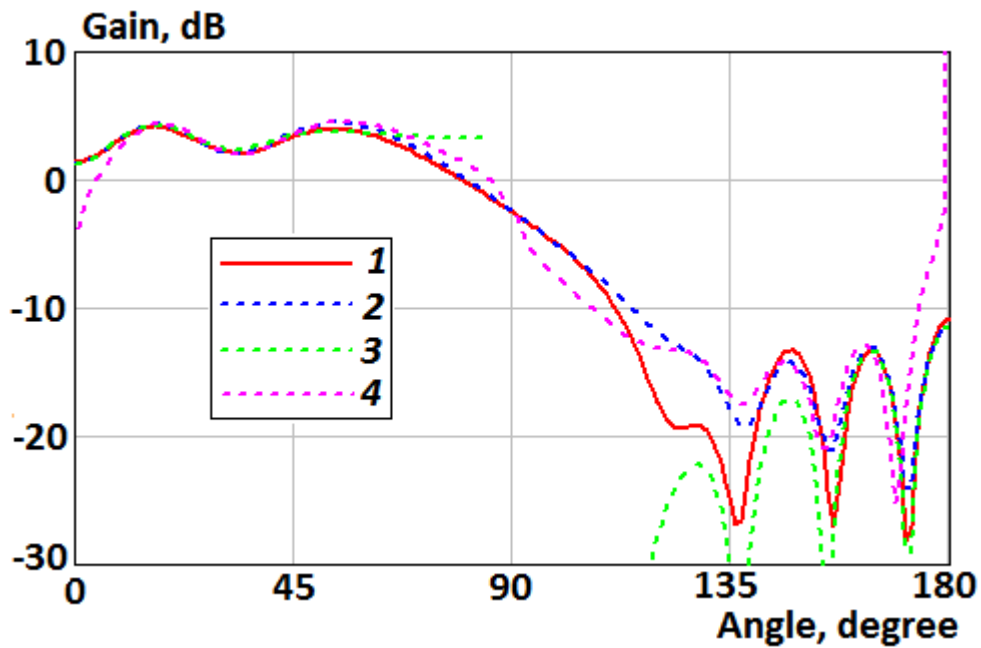


**Fig. 4.** Patterns of the parallel magnetic dipole mounted on the disk in  $E$ -plane: 1 – the numerical solution of the integral equation; 2 – the numerical integration of the Kirchhoff integral (formula (9)); 3 – the asymptotic formula (13); 4 – the asymptotic formula (18).

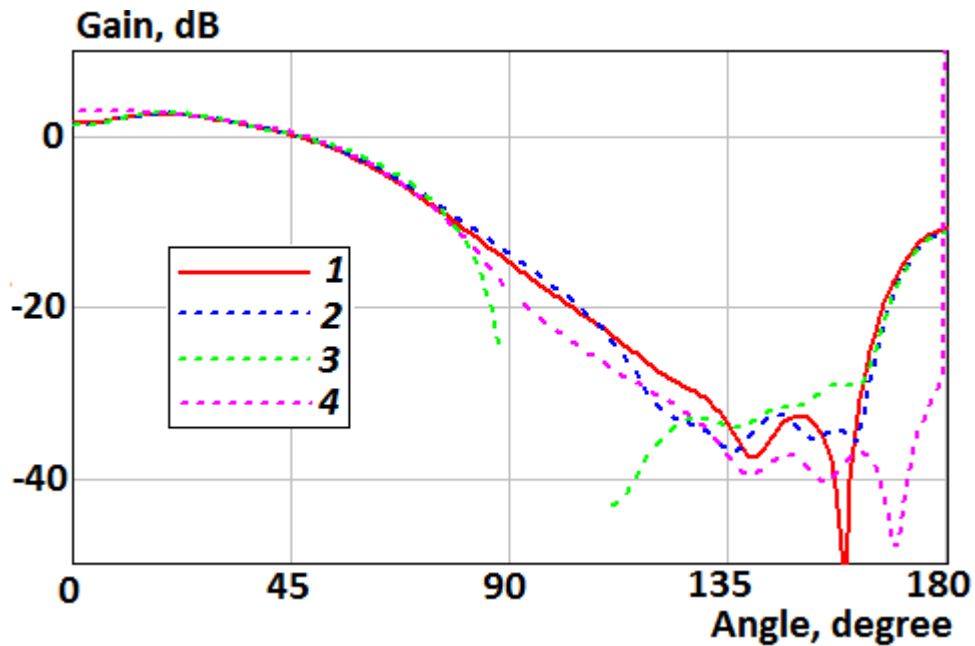


**Fig. 5.** Patterns of the parallel magnetic dipole mounted on the disk in  $H$ -plane: 1 – the numerical solution of the integral equation; 2 – the numerical integration of the Kirchhoff integral (formula (10)); 3 – the asymptotic formula (14); 4 – the asymptotic formula (19)

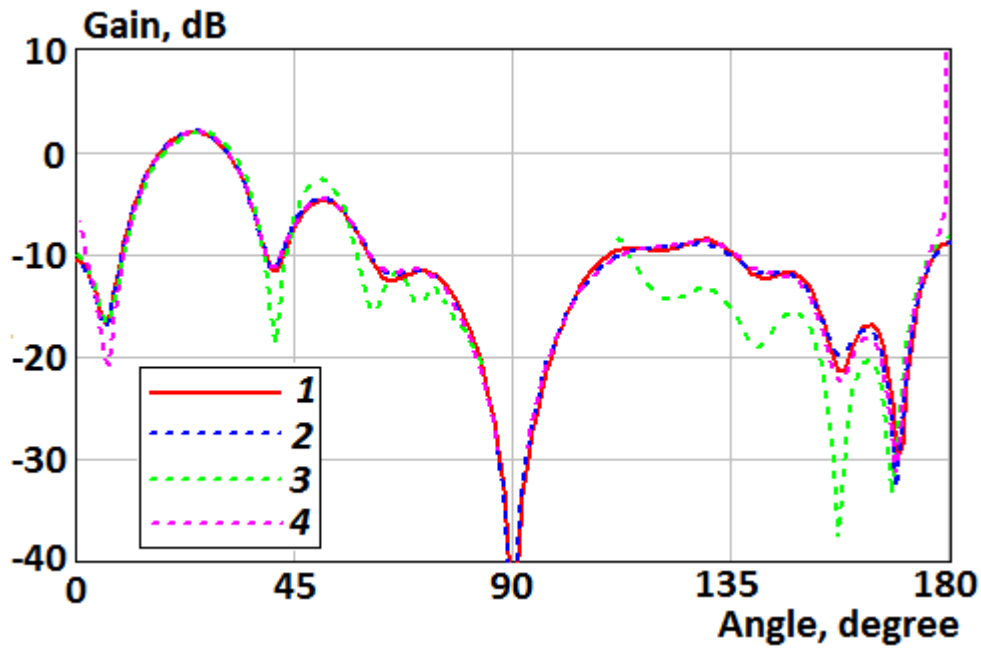


**Fig. 6.** Patterns of the parallel electric dipole above the disk in  $E$ -plane: 1 – the numerical solution of the integral equation; 2 – the numerical integration of the Kirchhoff integral (formula (9)); 3 – the asymptotic formula (13); 4 – the asymptotic formula (18)

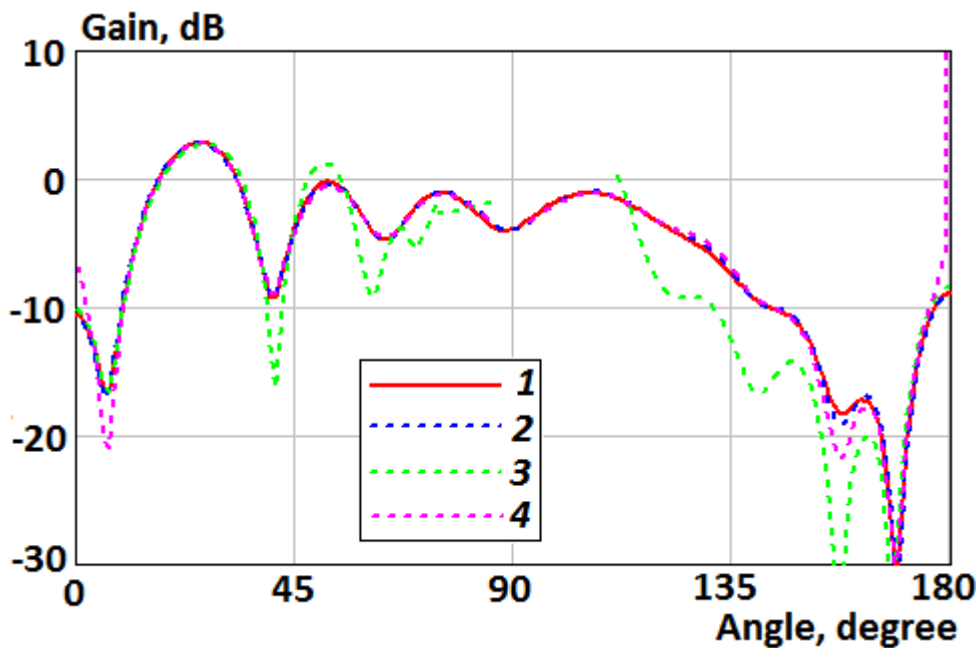


**Fig. 7.** Patterns of the parallel electric dipole above the disk in  $H$ -plane: 1 – the numerical solution of the integral equation; 2 – the numerical integration of the Kirchhoff integral (formula (10)); 3 – the asymptotic formula (14); 4 – the asymptotic formula (19)

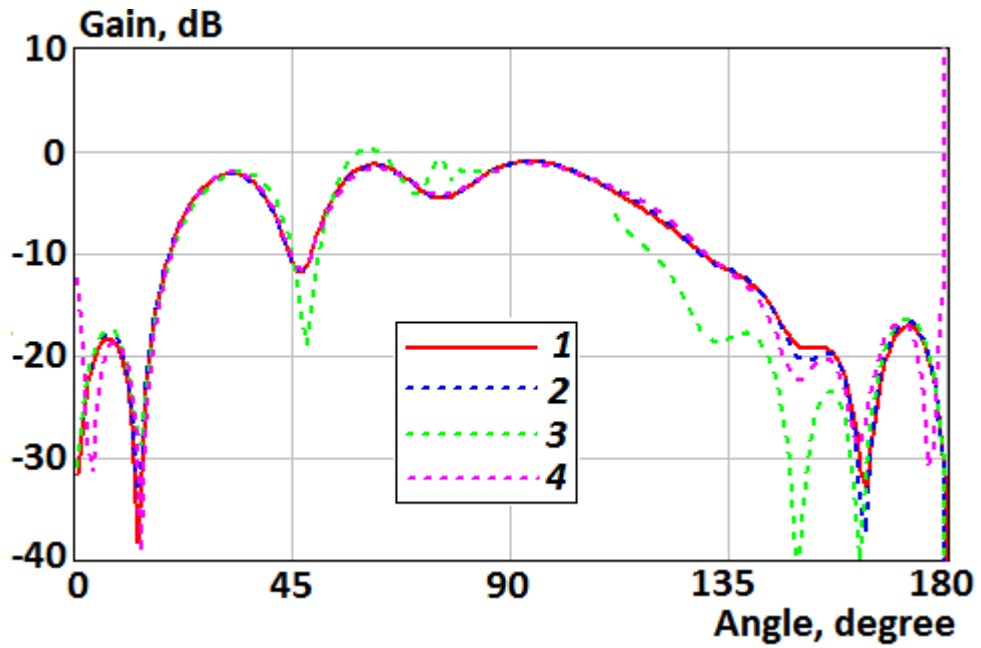


**Fig. 8.** Patterns of the perpendicular magnetic dipole above the disk: 1 – the numerical solution of the integral equation; 2 – the numerical integration of the Kirchhoff integral (formula (10)); 3 – the asymptotic formula (14); 4 – the asymptotic formula (19)

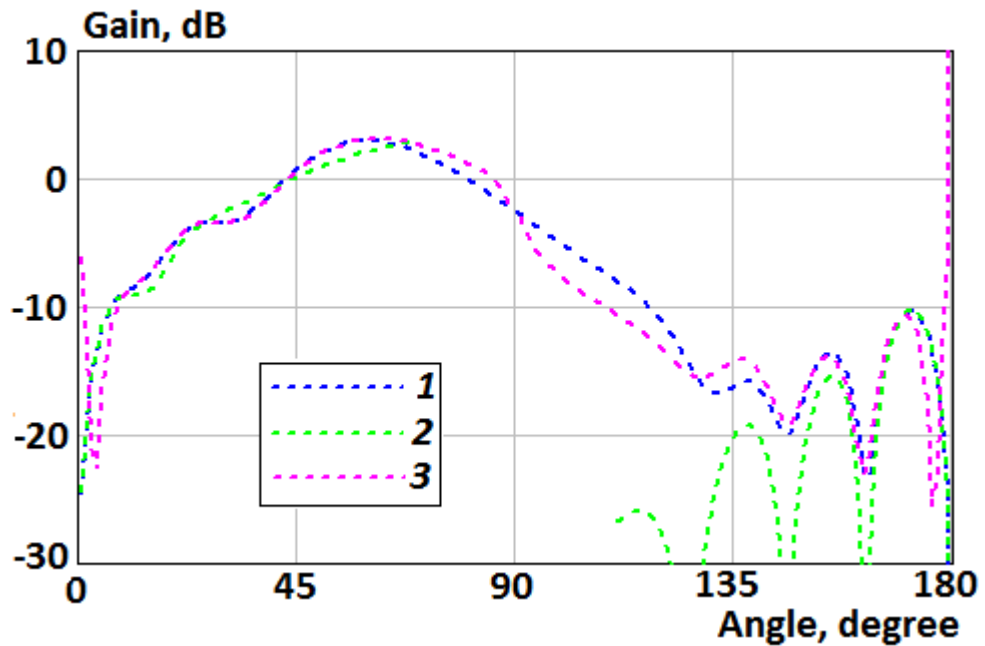


**Fig. 9.** Patterns of the perpendicular electric dipole mounted on the disk: 1 – the numerical integration of the Kirchhoff integral (formula (9)); 2 – the asymptotic formula (13); 3 – the asymptotic formula (18)

Figures 4-9 show that Kirchhoff approximation has good agreement with the numerical solution of integral equation. Also, the asymptotic formulas (18), (19) are good everywhere besides  $\theta < 10^\circ$  and  $\theta > 170^\circ$ , and formulas (13), (14) are good in these regions. It make possible to calculate scattering fields in full space using formulas (13), (14), (18), (19).

### 7. Sample of optimization

Let us optimize transparency of a disk of radius  $R=2\lambda$  to reduce the back radiation of a parallel magnetic dipole located on distance  $h=0.05\lambda$  above the disk. We consider two goal parameters which are determined as a ratio of mean-square power in lower hemisphere of a disk to mean-square power in upper hemisphere in  $E$ - and  $H$ -plane. The goal parameter writes for  $E$ - and  $H$ -plane, respectively, as

$$I^\phi = \frac{\int_{\theta=\pi/2}^{\pi} \left| H_\phi^\Sigma \left( r, \theta, \phi = \frac{\pi}{2} \right) \right|^2 d\theta}{\int_{\theta=0}^{\pi/2} \left| H_\phi^\Sigma \left( r, \theta, \phi = \frac{\pi}{2} \right) \right|^2 d\theta}, \quad (32)$$

and

$$I^\theta = \frac{\int_{\theta=\pi/2}^{\pi} \left| H_\theta^\Sigma (r, \theta, \phi = 0) \right|^2 d\theta}{\int_{\theta=0}^{\pi/2} \left| H_\theta^\Sigma (r, \theta, \phi = 0) \right|^2 d\theta}. \quad (33)$$

In (32), (33) the asymptotic representations of  $H_\phi^\Sigma(r, \theta, \phi)$  and  $H_\theta^\Sigma(r, \theta, \phi)$  are used and it assumes that  $r \rightarrow \infty$ . It was assumed that the disk is perfectly conducting in its center (i.e.  $\tau_\phi^H(0)=0, \tau_\rho^H(0)=0$  and  $\eta_\phi^H(0)=1, \eta_\rho^H(0)=1$ ). This condition allows to apply results to patch antennas with perfectly conducting ground.

The goal parameters are minimized by optimization of magnitudes of reflection coefficients  $\eta_\rho^H(\rho)$ ,  $\eta_\phi^H(\rho)$  and transmission coefficients  $\tau_\rho^H(\rho)$ ,  $\tau_\phi^H(\rho)$  using the gradient optimization method for purpose of reducing the back radiation in lower

hemisphere. The optimal distributions of magnitude of reflection and transmission coefficients and components of tensor (23) are shown in fig. 10, 11. We supposed the argument of these coefficients is zero. Distribution of magnitude of reflection and transmission coefficients  $\eta_{\phi}^H(\rho)$ ,  $\tau_{\phi}^H(\rho)=1-\eta_{\phi}^H(\rho)$  and  $\eta_{\rho}^H(\rho)$ ,  $\tau_{\rho}^H(\rho)=1-\eta_{\rho}^H(\rho)$  is shown in fig. 10. Distribution of magnitude of tensor's component  $Z_{rr}(r)$  and  $Z_{\phi\phi}(r)$  is shown in fig. 11. These magnitudes are normalized to  $W_0$ .

Figures 12 and 13 show patterns of the parallel magnetic dipole located above the semitransparent disk of radius  $R=2\lambda$  with the optimal transparency in  $E$ -plane  $H_{\phi}^{\Sigma}\left(r, \theta, \phi = \frac{\pi}{2}\right)$  and  $H$ -plane  $H_{\theta}^{\Sigma}(r, \theta, \phi = 0)$ , respectively. These figures show curves of the numerical solution of the integral equation for the semitransparent disk and perfectly conducting disk of the same radius.

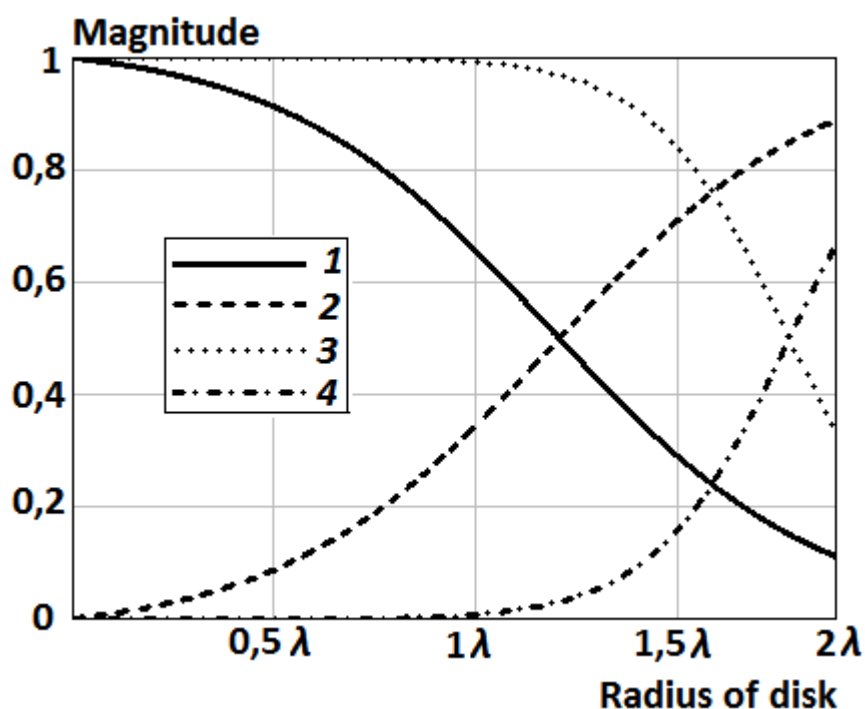


**Fig. 10.** The distribution of the magnitude of reflection and transmission coefficients on the disk's surface: 1 – magnitude of the reflection coefficient  $\eta_{\phi}^H(\rho)$ ; 2 –

magnitude of the transmission coefficient  $\tau_\phi^H(\rho)$ ; 3 – magnitude of the reflection coefficient  $\eta_\rho^H(\rho)$ ; 4 – magnitude of the transmission coefficient  $\tau_\rho^H(\rho)$

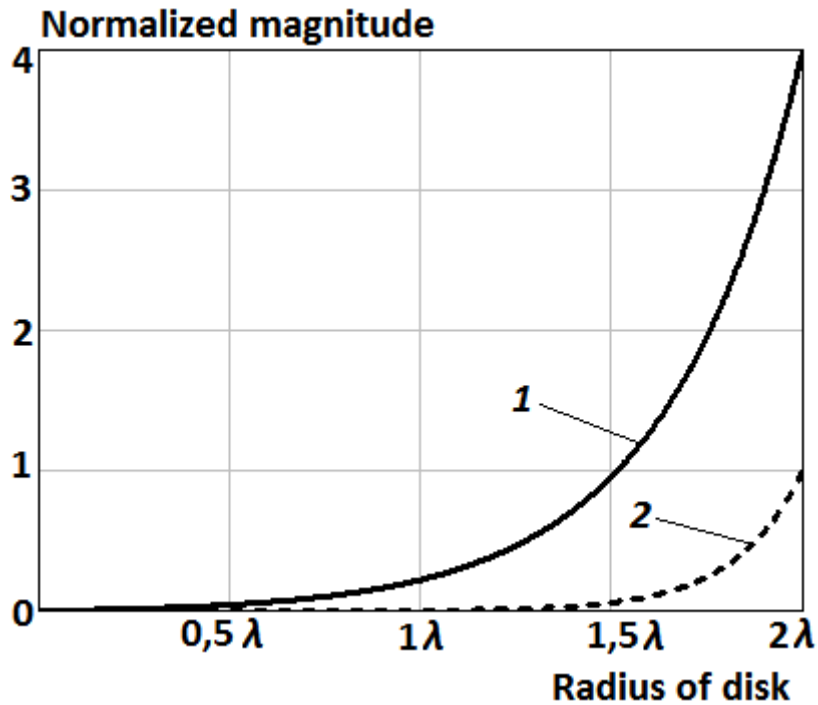


**Fig. 11.** The distribution of components of the impedance tensor (23) on the disk's surface: 1 – normalized magnitude of  $Z_{rr}(r)$ ; 2 – normalized magnitude of  $Z_{\phi\phi}(r)$

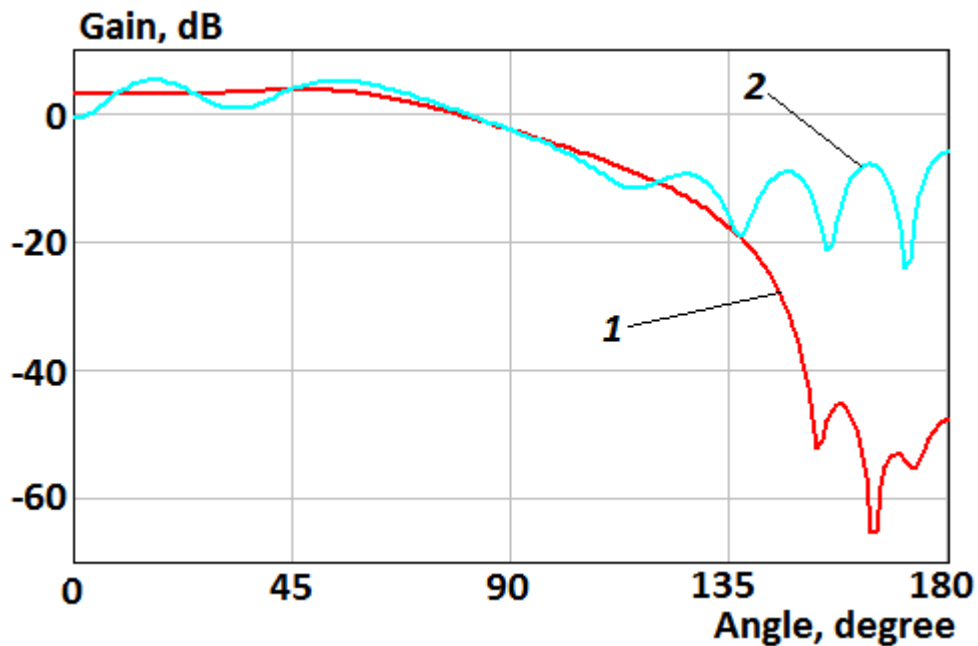


**Fig. 12.** Patterns of the parallel magnetic dipole located above the disk in  $E$ -plane: 1 – the semitransparent disk; 2 – the perfectly conducting disk

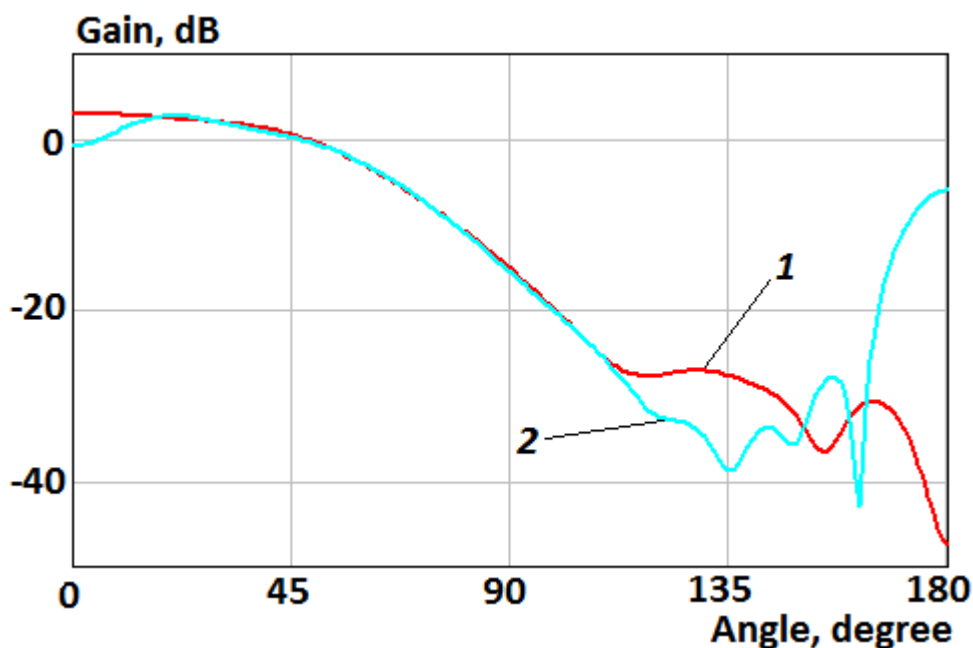


**Fig. 13.** Patterns of the parallel magnetic dipole located above the disk in  $H$ -plane: 1 – the semitransparent disk; 2 – the perfectly conducting disk

Figures 12, 13 show that radiation of parallel magnetic dipole in the lower hemisphere is reduced when transparency increases from center to edge of the disk as well as argument of coefficients of reflection and transmission and components  $Z_{rr}(r)$  and  $Z_{\phi\phi}(r)$  of impedance tensor (23) is zero. The front-to-back ratio of the parallel magnetic dipole in this case is 50.9 dB and 5.2 dB for the semitransparent and perfectly conducting disk, respectively.

### Conclusions

Asymptotic expressions for scattering field of an arbitrarily oriented magnetic and electric dipole located on axis of a semitransparent disk were obtained. Formulas for the front-to-back ratio for dipoles oriented parallel to the disk were presented.

Distribution of transparency for the radius of a disk  $2\lambda$  was optimized which provide significant reducing of back radiation of parallel magnetic dipole above the disk.

## References

1. *Leitner A., Spence R. D.* Effect of a Circular Ground Plane on Antenna Radiation // Journ. of Appl. Physics. Oct. 1950. V. 21. №10. pp. 1001–1006.
2. *Storer J. E.* The Radiation Pattern of an Antenna over a Circular Ground Screen // Journ. of Appl. Physics. May 1952. V. 23. №5. pp. 588–593.
3. *Tang C. L.* On the Radiation Pattern of a Base-Driven Antenna Over a Circular Conducting Screen // Journal of the Society for Industrial and Applied Mathematics. Dec. 1962. V. 10. № 4. 695–708.
4. *Keller J. B.* The field of an antenna near the center of a large circular disk // Journal of the Society for Industrial and Applied Mathematics. Dec. 1963. V. 11. № 4. 1110–1112.
5. *Lopez A. R.* The geometrical theory of diffraction applied to antenna pattern and impedance calculation // IEEE Trans. on Anten. and Prop. V. AP-14. № 1. Jan. 1966. pp. 40–45.
6. *Sang-Bin Rhee* Monopole Antenna with a Finite Ground Plane in the Presence of an Infinite Ground // Supplemental technical report. Nov. 1967. URL: <http://www.dtic.mil/dtic/tr/fulltext/u2/a007269.pdf>.
7. *Hahn K.F., Fikioris J.G.* Impedance and Radiation Pattern of Antennas above Flat Discs // IEEE Trans. Jan. 1973. V. AP-21. № 1. pp. 97–100.
8. *Awadalla K.H., Maclean T.S.M.* Monopole Antenna at Center of Circular Ground Plane: Input Impedance and Radiation Pattern // IEEE Trans. March 1979. V. AP-27. № 2. pp. 151–153.
9. *Richmond J. H.* Monopole antenna on circular disk // IEEE Trans. on Anten. and Prop. V. AP-32. № 12. Dec. 1984. pp. 1282–1287.
10. *Weiner M. M., Cruze S. P., Li Cho-Chou and Wilson W. J.* Monopole elements on circular ground planes. Northwood, MA: Artech House. 1987.
11. *Ibrahim H. M., Stephenson D. T.* Radiation patterns of a  $\lambda/4$  monopole mounted on thick finite square and circular ground planes // International Journal of Electronics. 1988. V. 64. № 3. pp. 345–358.
12. *Ibrahim H. M.* Radiation patterns of a  $\lambda/4$  monopole mounted on a small thick

- circular disc // International Journal of Electronics. 1990. V. 68. № 2. pp. 283–292.
13. *Weiner M. M.* Monopole antennas. New York, NY: Marcel Dekker. 2003.
  14. *Zivkovic Z., Senic D., Bodendorf C., Skrzypczynski J., Sarolic A.* Radiation pattern and impedance of a quarter wavelength monopole antenna above a finite ground plane // In proc. of 20-th International Conference on Software, Telecommunications and Computer Networks (SoftCOM). 2012.
  15. *Lusekelo Kibona* Impact of finite circular ground plane on the radiation patterns of the monopole antenna // International Journal of Software & Hardware Research in Engineering. Dec. 2013. V. 1. № 4. pp. 10–16. URL: [http://ijshre.com/wp-content/uploads/2013/12/IJSHRE\\_1412.pdf](http://ijshre.com/wp-content/uploads/2013/12/IJSHRE_1412.pdf).
  16. *Kishk A.A., Shafai L.* The Effect of Various Parameters of Circular Microstrip Antennas on Their Radiation Efficiency and the Mode Excitation // IEEE Trans. August 1986. V. AP-34. № 8. pp. 969–976.
  17. *Bhattacharyya A.K.* Effects of Finite Ground Plane on the Radiation Characteristics of a Circular Patch Antenna // IEEE Trans. February 1990. V. AP-38. № 2. pp. 152–159.
  18. *Noghanian S., Shafai L.* Control of microstrip antenna radiation characteristics by ground plane size and shape // IEE Proceedings Microwaves, Antennas and Propagation. June 1998. V. 145. № 3. pp. 207–212.
  19. *Lolit Kumar Singh L., Bhaskar Gupta, Partha P. Sarkar* Effects of Different Shaped and Size Ground Planes for Different Shaped Patch Antennas Characteristics // International Journal on Recent Trends in Engineering & Technology. Nov. 2010. V. 4. № 3. pp. 17–21.
  20. *Saeed I. Latif, Shafai L.* Pattern Equalization of Circular Patch Antennas Using Different Substrate Permittivities and Ground Plane Sizes // IEEE Trans. Oct. 2011. V. AP-59. № 10. pp. 3502–3511.
  21. *Клионовски К. К.* Характеристики направленности проводящих экранов круглой формы // Антенны. 2011. № 12. С. 31–37.

22. *Kaloshin V. A., Klionovski K. K.* Scattering of dipole field by perfectly conducting disk // Journal of radio electronics. 2013. №.12. URL: <http://jre.cplire.ru/jre/dec13/7/text.pdf>.
23. *Ufimtsev P. Ya.* Diffraction of electromagnetic waves at black bodies and semitransparent plates // Radiophysics and Quantum Electronics. 1968. V. 11. № 6. pp. 527–538.
24. *Wang R.W., Liepa V.V.* Reduction of the edge diffraction of a circular ground plane by using resistive edge loading // Anten. and Propag. Soc. Int. Symp. June 1985. V. 23. pp. 769–771.
25. *Klionovski K. K.* Theoretical and Experimental Research of Diffraction on Round Semitransparent Ground Plane // IEEE Trans. on Anten. and Propag. 2013. vol. 61. № 6. pp. 3207–3215.
26. *Felsen L., Marcuvitz N.* Radiation and scattering of waves. Hoboken, New Jersey, USA: John Wiley & Sons. 2003.
27. *Lewis R. M.* Asymptotic theory of transients // in book «Electromagnetic Wave Theory», Part 2 (ed. J. Brown), New York, USA: Pergamon Press. 1967. p. 864.